The Journal of Adhesion, 81:1031–1048, 2005

ISSN: 0021-8464 print/1545-5823 online
DOI: 10.1080/00218460500310762

Taylor & Francis
Taylor & Francis Group

Model Glycol-Terminated Surfaces for Adhesion Resistance

Mathilde I. Béthencourt
David Barriet
Nathalie M. Frangi
T. Randall Lee
Department of Chemistry, University of Houston,
Houston, Texas, USA

This manuscript introduces a new family of cyclic acetal-terminated alkanethiols used to prepare self-assembled monolayers (SAMs) on gold. The new SAMs, which are designed as variants of the biocompatible protein-repellant surfaces generated from thin films of oligoethylene glycol (OEG) or polyethylene glycol (PEG), were characterized by ellipsometry, contact-angle goniometry, and polarization modulation infrared reflection absorption spectroscopy (PM-IRRAS). A preliminary study of protein adhesion was also performed using fibrinogen as a model protein. The interfacial structure and properties of the new SAMs were compared with those generated from OEG-terminated alkanethiols and from surface-grafted PEG, which have been described previously. The data show that the new adsorbates form well packed and conformationally ordered films with contact angles of water ranging from 67° to 95°, depending on the precise structure of the acetal terminus. As a whole, the new SAMs offer a unique strategy for studying and designing adhesion-resistant biocompatible inferfaces.

Keywords: Glycol; Gold; Protein-resistant; SAMs; Self-assembled monolayers; Surfaces

INTRODUCTION

Since the early 1980s, polyethylene glycols (PEGs) have been widely used as surface coatings to resist the adsorption of proteins and

Received 29 September 2004; in final form 27 May 2005.

One of a collection of papers honoring Manoj Chaudhury, the February 2005 recipient of The Adhesion Society Award for Excellence in Adhesion Science, sponsored by 3M.

The Robert A. Welch Foundation (Grant No. E-1320) and the National Science Foundation (NIRT Award ECS-0404308) provided generous support for this research.

Address correspondence to T. Randall Lee, Department of Chemistry, University of Houston, 4800 Calhoun Road, Houston, TX 77204-5003, USA. E-mail: trlee@uh.edu

cells [1]. In biochemistry, biology, and medicine, PEG-coated surfaces are used because surfaces that repel proteins are needed, for example, as substrates for cell culture [2, 3] and as coatings for implants and contact lenses [4]. In the early 1990s, de Gennes argued that steric repulsion was responsible for the protein resistance imparted by high-molecular-weight PEGs [5]. These studies found that a high surface-chain density and a long PEG chain length are keys to optimal protein resistance.

In efforts to understand the mechanism by which PEG coatings create an antibioadhesive barrier, other researchers have attempted to outline the factors responsible for inhibiting the interaction between proteins and PEG chains. To this end, Whitesides and coworkers introduced the use of self-assembled monolayers (SAMs) of oligoethylene glycols (OEGs) on gold as interfacial PEG mimics [6]. These thiol-based monolayers offer the advantage of having a specific molecular composition and, thus, a well-defined chain length and packing structure. Even though the conformational freedom of OEG SAMs is markedly reduced compared with typical PEG-coated surfaces, initial studies found that the OEG monolayers also show excellent protein-resistant properties [6, 7]. Moreover, by systematically varying the number of repeat units in the OEG chain, it was determined that a minimum of two consecutive ethylene glycol moieties is necessary to achieve protein resistance [7].

SAMs are now widely used to study the interactions between biomaterials and organic surfaces. For example, Zhu and coworkers explored the relationship between OEG chain length and resistance to protein and cell adsorption [8]; Harder *et al.* examined the correlation between protein resistance and the molecular conformation of OEG-terminated thiols on gold and silver [9]; and Liedberg and coworkers studied the adhesion of fibrinogen, heparinized plasma, and serum to various OEG-terminated alkanethiols on gold [10].

A different approach to study the protein resistance of PEG coatings involves the grafting of PEG chains onto a surface, such as silicon [11] or gold [12]. This technique is derived from research involving polymer brushes, as described by Milner [13], who found that the efficacy of the brushes toward protein resistance was a function of the grafting density and the brush thickness. Theoretical studies conducted on the system by Halperin [14] showed that the interaction depended on the size of the protein being adsorbed. In the case of small proteins, high grafting density was needed to prevent adhesion onto the underlying substrate. In the case of large proteins, large brushes were needed to damp the van der Waals interactions between the proteins and the underlying substrate. These studies were consistent with

earlier work by Sofia [11], who concluded that the spaces between bound PEG chains should be smaller than the effective size of the protein.

Prior to the work reported here, studies utilizing OEG SAMs have consisted of films in which the OEG chains are oriented perpendicular (or nearly perpendicular) to the surface. Furthermore, studies have shown that conformation of the OEG moiety strongly influences the adhesion of proteins [9]. On gold, for example, the OEG chains exhibit a helical conformation [15] and resist protein adsorption; on silver, however, the OEG chains exhibit an "all trans" conformation and adsorb proteins. The ethylene glycol units of PEGs grafted onto surfaces are deprived of any predominant orientation with respect to the surface normal. The adhesion resistance of these surfaces depends largely on the concentration and size of the PEG moieties [16]. When taken as a whole, however, the previous studies reported in references 5–16 fail to provide a definitive answer regarding the relationship between protein resistance and glycol structure/orientation.

In an effort to explore this issue and to develop new classes of protein-resistant surfaces, we have synthesized a series of cyclic acetal-terminated alkanethiols for use in generating structurally and conformationally defined glycol interfaces (Figure 1). Because thin films produced by self-assembly are typically well packed and well organized [17], this approach should afford a high density of glycol units at the surface without the possibility of "holes" into which proteins of portions of proteins can insert. Another advantage is that the substituents on the cycle can be conveniently modified through organic synthesis to tailor the properties of the surface in a controlled

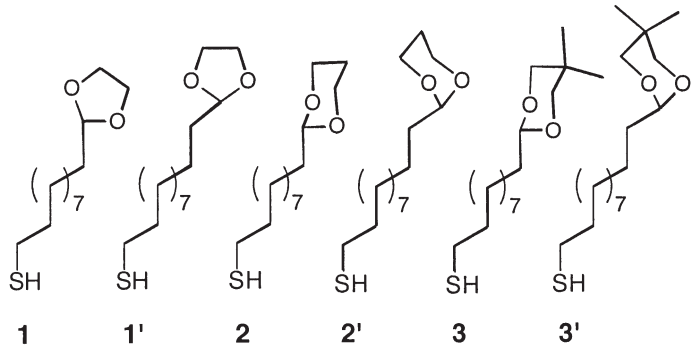

FIGURE 1 Structures of acetal-terminated alkanethiols used to generate SAMs on gold.

manner. In addition, the chain lengths of the underlying hydrocarbon linkers can be modified to dictate the orientation of the ring in a systematic "odd–even" fashion [18].

We report here the use of the new cyclic acetal-terminated thiols shown in Figure 1 to prepare SAMs on gold. These SAMs were characterized by ellipsometry, contact-angle goniometry, and polarization modulation infrared reflection absorption spectroscopy (PM-IRRAS). The analyses show that these adsorbates form densely packed and well-ordered SAMs in which the terminal glycol moiety is precisely positioned at the interface. The new SAMs offer a useful tool for studying the fundamental factors that govern the adhesion of cells and proteins to glycol-based surfaces.

EXPERIMENTAL

Synthesis of Adsorbates

The acetal-terminated alkanethiols were prepared as outlined in Scheme 1. The intermediates and products were characterized by NMR spectroscopy in $CDCl_3$ using a QE-300 spectrometer (300 MHz ^1H; 75 MHz ^{13}C; General Electric, Waukesha, WI, USA). The starting materials 10-undecenal, (Acros, Geel, Belgium) and 11-undecenyl bromide (TCI America, Tokyo, Japan) were purchased from the indicated suppliers, and 11-dodecenal was prepared as described in the following paragraph.

11-Dodecenal. An aliquot of 11-undecenyl bromide (6.02 g, 25.7 mmol) was dissolved in 40 mL of anhydrous diethyl ether and added to 1.85 g (76.0 mmol) of magnesium turnings with stirring. After the addition was complete, the reaction mixture was held at reflux for 2 h. Then, 4.19 g (28.3 mmol) of triethylorthoformate, purified by fractional distillation, were dissolved in 40 mL of anhydrous diethyl ether and added over a period of 1 h. The reaction mixture was held at reflux for an additional 5 h. Finally, the mixture was cooled to 0°C in an ice bath and stirred while 10% sulfuric acid was added slowly. The

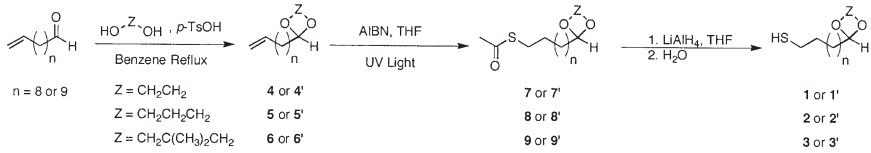

SCHEME 1 Synthetic route used to prepare the acetal-terminated alkanethiols.

organic layer was separated, and the aqueous phase was extracted four times with 20 mL of diethyl ether. The extract was dried over anhydrous magnesium sulfate, filtered, and evaporated under vacuum. Purification was achieved by column chromatography on silica gel with 2% diethyl ether in hexane as the eluant, which gave 11-dodecenal in 51% yield. ^{1}H NMR: δ 9.72 (t, $J = 1.8$ Hz, 1 H), 5.76–5.85 (m, 1 H), 4.91–5.02 (m, 2 H), 2.41 (dt, $J = 7.2$, 1.2 Hz, 2 H), 2.04 (m, 2 H), 1.62 (m, 2 H), 1.22 (br s, 12 H).

2-(Dec-9-enyl)-[1,3]-dioxolane (***4***). Aliquots of 10-undecenal (1.50 g, 8.23 mmol), ethylene glycol (766 mg, 12.3 mmol), and *p*-toluenesulfonic acid (*p*-TsOH) (142 mg, 0.825 mmol) were combined in benzene (100 mL) and left at reflux for 48 h with a Dean–Stark trap to remove water. The solvent was evaporated, and the residue was purified by column chromatography on silica gel using 2% diethyl ether in hexane as the eluant to give pure **4** in 87% yield. ^{1}H NMR: δ 5.74–5.84 (m, 1 H), 4.82–5.01 (m, 2 H), 4.90 (t, $J = 4.8$ Hz, 1 H), 3.81–3.99 (m, 4 H), 2.02 (m, 2 H), 1.56 (m, 2 H), 1.26 (br s, 12 H).

2-(Undec-10-enyl)-[1,3]-dioxolane (***4′***). This compound was prepared by the method used to prepare **4** but utilized 11-dodecenal as the starting aldehyde. ^{1}H NMR: δ 5.76–5.86 (m, 1 H), 4.84–5.02 (m, 2 H), 4.92 (t, $J = 5.1$ Hz, 1 H), 3.81–3.99 (m, 4 H), 2.02 (m, 2 H), 1.59 (m, 2 H), 1.26 (br s, 14 H).

2-(Dec-9-enyl)-[1,3]-dioxane (***5***). This compound was prepared by the method used to prepare **4** but utilized 1,3-propanediol as the starting diol. ^{1}H NMR: δ 5.77–5.82 (m, 1 H), 4.90–5.02 (m, 2 H), 4.53 (t, $J = 4.8$ Hz, 1 H), 4.10 (m, 2 H), 3.77 (dt, $J = 12.0$, 1.8 Hz, 2 H), 2.10 (m, 2 H), 2.06 (m, 2 H), 1.56 (m, 2 H), 1.29 (br s, 12 H).

2-(Undec-10-enyl)-[1,3]-dioxane (***5′***). This compound was prepared by the method used to prepare **4** but utilized 11-dodecenal as the starting aldehyde and 1,3-propanediol as the starting diol. ^{1}H NMR: δ 5.76–5.81 (m, 1 H), 4.89–5.01 (m, 2 H), 4.51 (t, $J = 5.1$ Hz, 1 H), 4.11 (m, 2 H), 3.76 (dt, $J = 12.0$, 2.1 Hz, 2 H), 2.09 (m, 2 H), 2.04 (m, 2 H), 1.55 (m, 2 H), 1.31 (br s, 14 H).

2-(Dec-9-enyl)-5,5-dimethyl-[1,3]-dioxane (***6***). This compound was prepared by the method used to prepare **4** but utilized 2,2-dimethyl-propane-1,3-diol as the starting diol. ^{1}H NMR: δ 5.77–5.86 (m, 1 H), 4.91–5.02 (m, 2 H), 4.41 (t, $J = 4.8$ Hz, 1 H), 3.60 (d, $J = 12$ Hz, 2 H), 3.42 (d, $J = 10.5$ Hz, 2 H), 2.03 (m, 2 H), 1.63 (m, 2 H), 1.28 (br s, 12 H), 1.20 (s, 3 H), 0.72 (s, 3 H).

2-(Undec-10-enyl)-5,5-dimethyl-[1,3]-dioxane (***6′***). This compound was prepared by the method used to prepare **4** but utilized 11-dodecenal as the starting aldehyde and 2,2-dimethyl-propane-1,3-diol as the starting diol. ^{1}H NMR: δ 5.76–5.85 (m, 1 H), 4.89–5.01 (m, 2 H), 4.40

(t, $J = 4.8$ Hz, 1 H), 3.61 (d, $J = 11.1$ Hz, 2 H), 3.39 (d, $J = 10.8$ Hz, 2 H), 2.01 (m, 2 H), 1.62 (m, 2 H), 1.26 (br s, 14 H), 1.18 (s, 3 H), 0.71 (s, 3 H).

11-([1,3]-Dioxolan-2yl)-decylthioacetate (**7**). A mixture of **4** (1.00 g, 4.71 mmol), thioacetic acid (3.50 mL, 490 mmol), and AIBN (80.0 mg, 0.487 mmol) in THF (15 mL) was irradiated by UV light using a Hanovia medium-pressure mercury-vapor lamp (450 W). After 2 h, an additional aliquot of AIBN (80.0 mg) was added, and irradiation was continued for 3 h. The solvent was evaporated, and the residue was purified by column chromatography using 5% diethyl ether in hexane as the eluant to give thioacetate **7** in 70% yield. ^{1}H NMR: δ 4.84 (t, $J = 4.8$ Hz, 1 H) 3.96 (m, 2 H), 3.85 (m, 2 H), 2.86 (t, $J = 7.5$ Hz, 2 H), 2.32 (s, 3 H), 1.64 (m, 2 H), 1.55 (m, 2 H), 1.26 (br s, 14 H).

11-([1,3]-Dioxolan-2-yl)-undecylthioacetate (**7′**). This compound was prepared by the method used to prepare **7** but utilized **4′** as the starting material. ^{1}H NMR: δ 4.84 (t, $J = 5.1$ Hz, 1 H), 3.95 (m, 2 H), 3.84 (m, 2 H), 2.85 (t, $J = 7.2$ Hz, 2 H), 2.31 (s, 3 H), 1.63 (m, 2 H), 1.53 (m, 2 H), 1.24 (br s, 16 H).

11-([1,3]-Dioxan-2-yl)-decylthioacetate (***8***). This compound was prepared by the method used to prepare **7** but utilized **5** as the starting material. ^{1}H NMR: δ 4.52 (t, $J = 5.1$ Hz, 1 H), 4.10 (dd, $J = 11.4$, 5.1 Hz, 2 H), 3.76 (dt, $J = 12.0$, 1.8 Hz, 2 H), 2.85 (t, $J = 7.5$ Hz, 2H), 2.33 (s, 3 H), 2.10 (m, 2 H), 1.57 (m, 4 H), 1.25 (br s, 14 H).

11-([1,3]-Dioxan-2-yl)-undecylthioacetate (***8′***). This compound was prepared by the method used to prepare **7** but utilized **5′** as the starting material. ^{1}H NMR: δ 4.51 (t, $J = 5.1$ Hz, 1 H), 4.09 (dd, $J = 10.2$, 4.8 Hz, 2 H), 3.76 (dt, $J = 12.0$, 2.1 Hz, 2 H), 2.85 (t, $J = 7.8$ Hz, 2 H), 2.32 (s, 3 H), 2.09 (m, 2 H), 1.56 (m, 4 H), 1.24 (br s, 16 H).

11-(5,5-Dimethyl-[1,3]-dioxan-2-yl)-decylthioacetate (***9***). This compound was prepared by the method used to prepare **7** but utilized **6** as the starting material. ^{1}H NMR: δ 4.40 (t, $J = 4.8$ Hz, 1 H), 3.59 (d, $J = 11.1$ Hz, 2 H), 3.35 (d, $J = 10.2$ Hz, 2 H), 2.86 (t, $J = 7.5$ Hz, 2 H), 2.33 (s, 3 H), 1.51–1.62 (m, 4 H), 1.24 (br s, 14 H), 1.19 (s, 3 H), 0.72 (s, 3 H).

11-(5,5-Dimethyl-[1,3]-dioxan-2-yl)-undecylthioacetate (***9′***). This compound was prepared by the method used to prepare **7** but utilized **6′** as the starting material. ^{1}H NMR: δ 4.40 (t, $J = 4.8$ Hz, 1 H), 3.61 (d, $J = 10.8$ Hz, 2 H), 3.39 (d, $J = 10.8$ Hz, 2 H), 2.85 (t, $J = 7.5$ Hz, 2 H), 2.30 (s, 3 H), 1.55–1.61 (m, 4 H), 1.26 (br s, 16 H), 1.18 (s, 3 H), 0.71 (s, 3 H).

11-([1,3]-Dioxolan-2-yl)-decanethiol (***1***). Before use, thioacetate **7** was dissolved in diethyl ether and washed with sodium bicarbonate. An aliquot of **7** (2.00 g, 7.69 mmol) was then dissolved in 20 mL of

dry diethyl ether and added to 584 mg (15.4 mmol) of $LiAlH_4$ in 40 mL of dry diethyl ether. The mixture was stirred at rt under argon for 6 h. Water was added until no more bubbling was observed. The mixture was extracted four times with 20 mL of diethyl ether. The organic layer was dried over anhydrous magnesium sulfate and filtered, and the volatiles were removed under vacuum. The residue was purified by column chromatography (8% diethyl ether in hexanes) to afford **1** in 71% yield. ^{1}H NMR: δ 4.83 (t, $J = 4.8$ Hz, 1 H), 3.96 (m, 2 H), 3.86 (m, 2 H), 2.51 (m, 2 H), 1.64 (m, 2 H), 1.52 (m, 2 H), 1.25 (br s, 14 H).

11-([1,3]-Dioxolan-2-yl)-undecanethiol (***1′***). This compound was prepared by the method used to prepare **1** but utilized **7′** as the starting material. ^{1}H NMR: δ 4.84 (t, $J = 5.1$ Hz 1 H), 3.97 (m, 2 H), 3.86 (m, 2 H), 2.51 (m, 2 H), 1.63 (m, 2 H), 1.53 (m, 2 H), 1.26 (br s, 16 H).

11-([1,3]-Dioxan-2-yl)-decanethiol (***2***). This compound was prepared by the method used to prepare **1** but utilized **8** as the starting material. ^{1}H NMR: δ 4.50 (t, $J = 5.4$ Hz 1 H), 4.10 (dd, $J = 10.2$, 4.8 Hz, 2 H), 3.75 (dt, $J = 12.6$, 3.0 Hz, 2 H), 2.51 (m, 2 H), 2.07 (m, 2 H), 1.56 (m, 4 H), 1.25 (br s, 14 H).

11-([1,3]-Dioxan-2-yl)-undecanethiol (***2′***). This compound was prepared by the method used to prepare **1** but utilized **8′** as the starting material. ^{1}H NMR: δ 4.50 (t, $J = 4.8$ Hz 1 H), 4.09 (dd, $J = 10.8$, 5.1 Hz, 2 H), 3.76 (dt, $J = 12.3$, 2.7 Hz, 2 H), 2.51 (m, 2 H), 2.05 (m, 2 H), 1.58 (m, 4 H), 1.25 (br s, 16 H).

11-(5,5-Dimethyl-[1,3]-dioxan-2-yl)-decanethiol (***3***). This compound was prepared by the method used to prepare **1** but utilized **9′** as the starting material. ^{1}H NMR: δ 4.40 (t, $J = 4.8$ Hz, 1 H), 3.59 (d, $J = 11.4$ Hz, 2 H), 3.42 (d, $J = 10.8$ Hz, 2 H), 2.48–2.55 (m, 2 H), 1.55–1.63 (m, 4 H), 1.26 (br s, 14 H), 1.19 (s, 3 H), 0.71 (s, 3 H).

11-(5,5-Dimethyl-[1,3]-dioxan-2-yl)-undecanethiol (***3′***). This compound was prepared by the method used to prepare **1** but utilized **9′** as the starting material. ^{1}H NMR: δ 4.40 (t, $J = 4.8$ Hz, 1 H), 3.59 (d, $J = 11.1$ Hz, 2 H), 3.41 (d, $J = 11.4$ Hz, 2 H), 2.47–2.55 (m, 2 H), 1.54–1.65 (m, 4 H), 1.26 (br s, 16 H), 1.18 (s, 3 H), 0.71 (s, 3 H).

Preparation of SAMs

Ethanolic solutions of the thiols (1 mM) were prepared in vials previously cleaned with "piranha solution" (7:3 concentrated H_2SO_4/30% H_2O_2). *Caution: piranha solution reacts violently with organic materials and should be handled carefully*. The bottles were then rinsed successively with deionized water and ethanol and dried overnight at 100°C. Gold surfaces were prepared by the thermal

evaporation of chromium (*ca.* 100 Å) onto ethanol-washed silicon wafers, followed by the evaporation of gold (*ca.* 1000 Å). The resultant gold-coated wafers were cut into slides (*ca.* 1×3 cm), washed with absolute ethanol, and blown dry with nitrogen before being dipped into the respective thiol solutions and allowed to equilibrate for 24 h.

Measurements of Ellipsometric Thickness

The thicknesses of the monolayers were obtained with a Rudolf Research Auto EL III ellipsometer (Rudolf, Denville, NJ, USA) equipped with a He-Ne laser operating at 632.8 nm and an angle of incidence of 70° for effective protein resistance. Based on the latter hypothesis, we can expect SAMs derived from **1** and **1′**. To determine the thicknesses, we assumed a refractive index of 1.45 for all of the films. For each type of film, data were collected and averaged from measurements on four distinct slides using three separate spots per slide. The thicknesses for all of the SAMs were found to be reproducible within ±2 Å.

Contact-Angle Measurements

Contact angles were measured with a Ramé-Hart model 100 contact-angle goniometer (Ramé-Hart, Mountain Lakes, NJ, USA). The contacting liquids, hexadecane (HD), water (H_2O), acetonitrile (AC), N,N-dimethylformamide (DMF), methylformamide (MF), and formamide (FA), were of the highest purity available commercially. They were dispensed and withdrawn using a Matrix Technologies Micro-Electrapette 25 (Matrix Tech., Lowell, MA, USA). Contact angles were collected and averaged from measurements on four distinct slides using three separate drops per slide.

Polarization Modulation Infrared Reflection Absorption Spectroscopy (PM-IRRAS)

PM-IRRAS data were acquired using a Nicolet Magna-IR 860 Fourier-transform spectrometer (Nicolet, Madison, WI, USA) equipped with liquid nitrogen–cooled MCT detector and a PEM-90 photoelastic modulator operating at 37 kHz (Hinds Instruments, Hillsboro, OR, USA). The infrared light was reflected from the sample at an angle of incidence of 80°. The spectra were collected using 64 scans at a spectral resolution of 4 cm^{-1}.

Protein Adsorption Studies

The SAMS were removed from the solution in which they were prepared, rinsed thoroughly with ethanol, and blown dry with nitrogen. They were then immersed for 1 h in a solution containing 1 mg/mL of fibrinogen in 0.1 M aqueous PBS buffer at room temperature. The thickness of adsorbed protein layers that remained on the SAMs after rinsing with water was measured by ellipsometry as described in the literature [6, 7]. Fibrinogen adsorption on the different substrates was quantified relative to protein adsorption on monolayers of hexadecanethiol [19].

RESULTS AND DISCUSSION

Thicknesses of the Films

We compared the thicknesses of the films generated from the acetal-terminated molecules with those generated from normal alkanethiols having analogous chain lengths. Studies of ω-alkoxy-n-alkanethiolate monolayers on gold have found that the ether moieties fail to perturb the packing of the SAMs [20, 21]; as such, the observed ellipsometric thicknesses are comparable with SAMs derived from normal alkanethiols. Correspondingly, the length of compound **1** is most analogous to $CH_3(CH_2)_{12}SH$, **1**′ and **2** are analogous to $CH_3(CH_2)_{13}SH$, **2**′ and **3** are analogous to $CH_3(CH_2)_{14}SH$, and **3**′ is analogous to $CH_3(CH_2)_{15}SH$ (see Figure 1). Based on these assumptions, the data in Figure 2 show a progressive increase in thickness as the chain lengths are increased. Moreover, the thicknesses of the films derived from the acetal-terminated thiols are within 2 Å of the films derived from the proposed corresponding normal alkanethiols. The comparison is surprisingly good, given the additional steric bulk of the tailgroups, the multiple conformations available to the cyclic moieties at the interface, and the experimental error associated with ellipsometric measurements.

Wettabilities of the Films

Numerous studies in the literature have demonstrated the sensitivity of contact angles with regard to the composition, packing, and orientation of organic thin films [20–22]. Perhaps the most reliable way to interpret the wettability of new types of SAMs is to collect the contact angles using several different types of contacting liquids and compare the data with those obtained using a well-characterized family of adsorbates. In our case, we compared SAMs generated from the acetal-terminated alkanethiols with those derived from normal

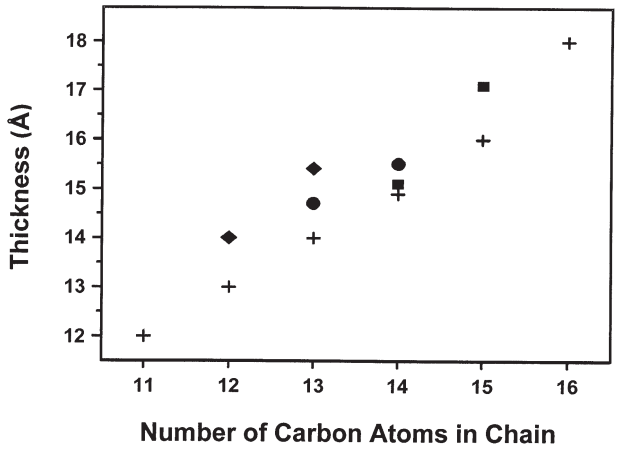

FIGURE 2 Comparison of the ellipsometric thickness of SAMs derived from the acetal-terminated alkanethiols with those derived from the corresponding normal alkanethiols: (+) normal alkanethiols, (◆) compounds **1** and **1′**, (●) compounds **2** and **2′**, and (■) compounds **3** and **3′**. The thickness values were reproducible to ±1 Å.

alkanethiols and those derived from OEG-terminated SAMs. The value of the advancing contact angle of water for hydroxy-terminated OEG SAMs of various chain lengths is approximately 38° [6]. In contrast, SAMs derived from **1** exhibit an advancing contact angle for water of 69° (see Table 1), reflecting the presence of the terminal methylene groups rather than a terminal hydroxyl group. The value of 69° is, however, markedly lower than that for normal alkanethiols SAMs

TABLE 1 Advancing Contact Angles and Hysteresis for SAMs on Gold Derived from the Acetal-terminated Alkanethiols

	Advancing contact angles, $\theta_a \pm 1°$ (hysteresis $\Delta\theta = \theta_a - \theta_r$)[a]					
Adsorbate	H_2O	HD	AC	DMF	MF	FA
1	69 (7)	11 (5)	23 (7)	25 (9)	37 (9)	59 (7)
1′	67 (7)	16 (6)	19 (7)	22 (7)	34 (9)	58 (8)
2	72 (5)	10 (5)	15 (3)	39 (5)	46 (7)	63 (7)
2′	73 (8)	10 (4)	15 (7)	32 (6)	46 (8)	62 (6)
3	93 (7)	30 (9)	51 (7)	63 (8)	67 (7)	84 (6)
3′	94 (10)	29 (8)	50 (7)	59 (6)	65 (7)	80 (6)

[a]The uniformly low values of hysteresis suggest homogeneous and smooth interfaces for all SAMs [31].

(115°), reflecting the presence of the oxygen atoms near the interface in these SAMs.

Upon progression from adsorbates **1** to **3**, it is reasonable to assume that the oxygen atoms will become progressively buried into the film. The advancing contact angles for water reflect this trend: 69° (**1**), 72° (**2**), and 93° (**3**), suggesting a systematic decrease in the interaction between water and the films. The wettability by water of SAMs derived from adsorbates **1′**, **2′**, and **3′** is consistent with these observations (see Table 1), suggesting no substantial changes in the interfacial composition or orientation as a function of odd *vs.* even chain length [18].

We note that the advancing contact angle of water on PEG-grafted surfaces is approximately 58° [23], and that for methoxy-terminated OEG SAMs is between 65° and 71° depending on the numbers of glycol units [19]. Consequently, the SAMs derived from **1–3** can perhaps be more appropriately compared with PEG-grafted surfaces and methoxy-terminated OEG SAMs rather than to hydroxy-terminated OEG SAMs. Moreover, according to Herrwerth *et al.* [19], higher terminal hydrophobicity leads to increased protein adsorption; specifically for OEG SAMs on gold, a water contact angle of $\leq 70°$ is required for effective protein resistance. Based on the latter hypothesis, we can expect SAMs derived from **1** and **1′** is required for effective protein resistance. Based on the latter hypothesis, we can expect SAMs derived from **1** and **1′** to be protein resistant ($\theta_a^{H_2O} \approx 68°$), SAMs derived from **2** and **2′** to be somewhat less protein resistant ($\theta_a^{H_2O} \approx 72°$), and SAMs derived from **3** and **3′** to be protein adsorbing ($\theta_a^{H_2O} \approx 93°$). Preliminary studies of the adsorption of fibrinogen to these SAMs support this trend (*vide infra*).

Water is a particularly useful contacting liquid for evaluating the potential for protein repellency because the manner in which it interacts with a surface reflects the arrangement of the aqueous boundary layer between the surface and proteins in solution. However, the cohesive energy of water is quite high [24], which inhibits its ability to interact fully with a substrate. As a consequence, the use of water alone as a probe liquid is insufficient to evaluate the structure of the upper layer of atoms (*i.e.*, the adsorbate tailgroups), which are largely responsible for the antiadhesive properties of the surface [19].

Hexadecane (HD) is a nonpolar aprotic contacting liquid commonly used to probe purely dispersive interactions at organic interfaces [25]. Table 1 shows that the contact angles of HD measured for all of the acetal-terminated films are substantially lower than those obtained on normal alkanethiols SAMs ($\sim 52°$) [21]. This difference reflects a combination of interfacial methylene groups and underlying oxygen atoms for the acetal-terminated SAMs in contrast to a mixture of interfacial methyl and methylene groups for the normal alkanethiols

SAMs. Similarly, we note that the SAMs derived from **3** and **3′**, which also expose a mixture of methyl and methylene groups at the interface, exhibit substantially higher advancing contact angles of HD than those of the other acetal-terminated SAMs.

The data in Table 1 further show that the polar aprotic contacting liquid acetonitrile (AC) mirrors the trends observed with HD, whereas the polar aprotic contacting liquid dimethylformamide (DMF) shows enhanced wettability on **1** and **1′** compared to **2** and **2′**. Furthermore, the polar protic contacting liquids methylformamide (MF) and formamide (FA) mirror the trends observed with DMF. It is important to note that all of the probe liquids indicate that the least-wettable SAMs are those derived from **3** and **3′**. Moreover, all of the probe liquids, excluding HD and AC, indicate that the SAMs derived from **2** and **2′** are less wettable than those derived from **1** and **1′**, which suggests that the discrepancy lies with the probe liquids HD and AC. As noted previously, it is possible that the discrepancy is due to intercalation phenomena. Future studies will attempt to address this issue.

Works of Adhesion

To probe the physical origins of the wettabilities of the acetal-terminated alkanethiol SAMs, we calculated the work of adhesion (W_{SL}) between the probe liquids and the surfaces of the SAMs using the modified Good–Girifalco–Fowkes relation ($W_{SL} = W^{d}_{SL} + W^{p}_{SL}$), which separates the components of the total work of adhesion (W_{SL}) into dispersive (W^{d}_{SL}) and polar (W^{p}_{SL}) parts [26–29]. With the approach, the works of adhesion can be calculated as follows: $W_{SL} = \gamma_L(1 + \cos\,\theta_a)$, $W^{d}_{SL} = 2(\gamma^{d}_{S}\gamma^{d}_{L})^{1/2}$, and $W^{p}_{SL} = W_{SL} - W^{d}_{SL}$. The value of γ^{d}_{S} can be estimated for each surface by using hexadecane as the probe liquid and assuming that $W_{SL} = W^{d}_{SL}$ [24, 30]. The literature values of γ_L [27] and the calculated values of γ^{d}_{L}, which were estimated for each probe liquid by using SAMs derived from normal alkanethiols [22, 27], are

TABLE 2 Values of Surface Tension ($mJ \cdot m^{-2}$) for the Various Contacting Liquids [20, 27]

Contacting liquid	γ_L ($mJ \cdot m^{-2}$)	γ^{d}_{L} ($mJ \cdot m^{-2}$)
Water (H_2O)	72.4	23.8
Hexadecane (HD)	27.5	27.5
Acetonitrile (AC)	27.0	19.3
Dimethylformamide (DMF)	36.8	30.0
Methylformamide (MF)	38.8	27.5
Formamide (FA)	58.0	33.5

TABLE 3 Work of Adhesion W_{SL} and the Dispersive and Polar Components of the Work of Adhesion W_{SL}^{d} and W_{SL}^{p} for Various Probe Liquids on SAMs Derived from the Acetal-Terminated Alkanethiols

	H_2O (W in mJ · m^{-2})			AC (W in mJ · m^{-2})			DMF (W in mJ · m^{-2})			MF (W in mJ · m^{-2})			FA (W in mJ · m^{-2})		
Adsorbate	W_{SL}	W_{SL}^{d}	W_{SL}^{p}	W_{SL}	W_{SL}^{d}	W_{SL}^{p}	W_{SL}	$W_{SL}{}^{d}$	W_{SL}^{p}	W_{SL}	W_{SL}^{d}	W_{SL}^{p}	W_{SL}	W_{SL}^{d}	W_{SL}^{p}
1	98.3	50.7	47.6	51.9	45.7	6.2	70.2	56.9	13.2	69.8	54.5	15.3	87.9	60.1	27.7
1′	100.7	50.2	50.5	52.5	45.2	7.3	70.9	56.3	14.6	71.0	53.9	17.0	88.7	59.5	29.2
2	94.8	50.8	44.0	53.1	45.7	7.4	65.4	57.0	8.4	65.8	54.6	11.2	84.3	60.2	24.1
2′	93.6	50.8	42.8	53.1	45.7	7.4	68.0	57.0	11.0	65.8	54.6	11.2	85.2	60.2	25
3	68.5	47.7	20.9	44.0	43.0	1.0	53.6	53.5	0.1	54.0	51.3	2.6	64.1	56.6	7.4
3′	67.3	48.0	19.4	44.4	43.2	1.2	55.8	53.8	1.9	55.2	51.6	3.6	68.1	56.9	11.2

provided in Table 2. Furthermore, Table 3 shows the various works of adhesion for the different adsorbates. For all probe liquids, the six adsorbates have comparable dispersive components of the work of adhesion, W_{SL}^{d}, but **3** and **3′** differ by their polar component, W_{SL}^{p}, which is much smaller than for the four others.

The observed similarities in the values of W_{SL}^{d} are reasonable, given that all adsorbates present similarly packed methylene and/or methyl moieties at the interface. In contrast, the relatively small value of W_{SL}^{p} observed for SAMs derived from **3** and **3′** is probably due to the fact that the oxygen atoms here are buried into the surface and are thus less available to interact with the probe liquids. For all adsorbates, the polar component of the work of adhesion is smaller in the case of polar aprotic solvents (AC and DMF), which highlights the potential importance of hydrogen-bonding in the interaction between the probe liquids and the substrate. Water, for example, displays the highest value of W_{SL}^{p}, followed by FA and MF, for which hydrogen bonding can plausibly be expected to decrease systematically.

Polarization Modulation Infrared Reflection Absorption Spectroscopy (PM-IRRAS)

Infrared reflectance spectra of the SAMs on gold derived from the acetal-terminated SAMs are shown in Figure 3. For all of the adsorbates, the methylene antisymmetric ($\nu_{as}^{CH_2}$) and methylene symmetric ($\nu_{s}^{CH_2}$) bands appear at roughly 2919 and 2850 cm^{-1}, respectively which is compatible with a well-packed and conformationally ordered structure for the methylene chains [31]. This hypothesis is supported by transmission IR studies of the neat compounds, where these bands appear at 2925 and 2850 cm^{-1}, respectively (data not shown). Furthermore, we observed no systematic variation for any of the band positions (methyl, methylene, or methine) as a function of odd *vs.* even chain length, suggesting that the terminal rings are conformationally flexible.

In the case of adsorbates **1** and **1′**, we observed an absorption at $\sim$2880 cm^{-1} due to the symmetric stretch of the methylene groups adjacent to the oxygen atoms ($\nu_{s}^{CH_{cycle}}$) [32]. We observed no corresponding antisymmetric band for these adsorbates, which should appear at 2955–2922 cm^{-1} [33]. We note, however, that we observed the $\nu_{as}^{CH_{cycle}}$ band for all the six-membered ring adsorbates (**2, 2′**, **3**, and **3′**). Because the $\nu_{s}^{CH_{cycle}}$ band corresponds to the shoulder observed on the $\nu_{as}^{CH_2}$ of the methylene backbone (see Figure 3), it is possible that the $\nu_{as}^{CH_{cycle}}$ band for **1** and **1′** is shifted because of ring strain and might be hidden by the relatively intense $\nu_{as}^{CH_2}$ band of the backbone. Alternatively, this vibration might be parallel to the surface for **1** and **1′** and

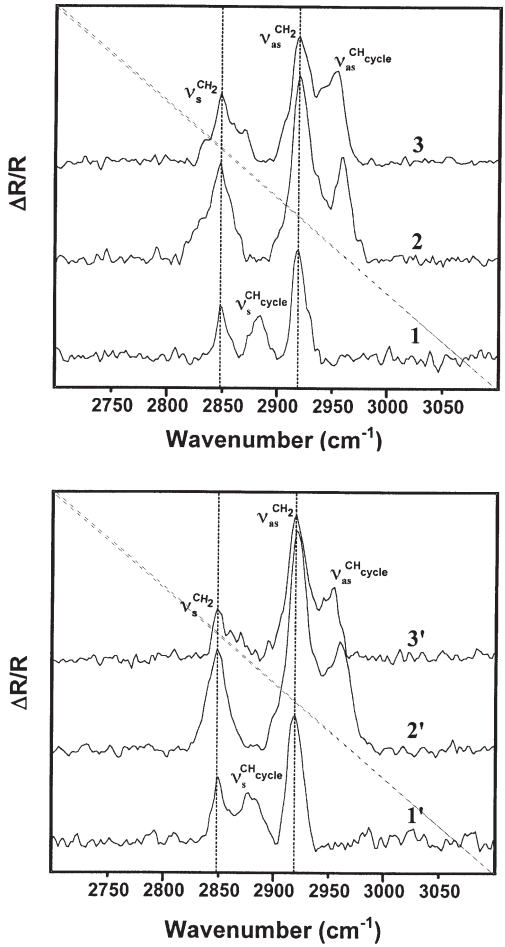

FIGURE 3 Surface infrared spectra (PM-IRRAS) of SAMs generated from the acetal-terminated alkanethiols.

thus be forbidden by surface selection rules [34]; this hypothesis is, however, not supported by transmission IR spectra of neat samples of **1** and **1′**, for which no $\nu_{as}^{CH_{cycle}}$ band can be discerned (data not shown). Conversely, although we observed the $\nu_{as}^{CH_{cycle}}$ for SAMs derived from **2** **2′**, **3**, and **3′**, we were unable to observe the $\nu_{s}^{CH_{cycle}}$ for SAMs derived from the adsorbates, which should appear at 2878–2835 cm^{-1} [33] and, thus, possibly obscured by the $\nu_{s}^{CH_2}$ band of the chain backbone. We note that transmission IR spectra of neat samples of these adsorbates also exhibited no discernable $\nu_{s}^{CH_{cycle}}$ band (data not shown).

For adsorbates **3** and **3′**, we would expect to see absorption bands for the methyl groups, which normally appear at 2960 cm^{-1} (methyl antisymmetric stretch, $\nu_{as}^{CH_3}$) and 2870 cm^{-1} (methyl symmetric stretch, $\nu_{s}^{CH_3}$). Both of these absorptions are expected to lie near the corresponding CH_2 bands and are, thus, difficult to resolve. We note, however, the presence of a shoulder at ~2870 cm^{-1} on the $\nu_{s}^{CH_2}$ band in the PM-IRRAS spectra, which might correspond to the $\nu_{s}^{CH_3}$ band because we did not observe this shoulder for SAMs derived from **2** and **2′**. As a whole, the PM-IRRAS data support the anticipated film structure and composition based on the specific adsorbate used.

Protein Adsorption

Using fibrinogen as a model protein, we briefly explored the protein resistance of the new acetal-terminated SAMs on gold. The data in Table 4 illustrate a trend on going from adsorbate **1** to **3**. It appears that as the oxygen atoms are buried into the film, the ability of the resulting surface to resist protein adsorption decreases, which is consistent with the hypothesis that the hydrophilicity/hydrophobicity of the terminal group is critical to the protein adhesion process [19]. The data are also consistent with the proposal by Jiang *et al.*, who contend that the number of hydrogen bonds between water and oxygen atoms in the glycol moieties influences the efficiency of protein resistance [35]. Nevertheless, the new substrates appear to be less protein resistant than their ethylene glycol and trimethylene glycol cousins [19]. Although the outer layer of the film obtained from **1** and **1′** appears analogous to the structure of ethylene glycol (OCH_2CH_2O), the percentage of fibrinogen adsorption is more comparable with that observed on SAMs terminated with ethoxyethylene glycol ($HS-(CH_2)_{11}-(O-CH_2-CH_2)_6-OEt$) [19]. This comparison is somewhat surprising considering that the oxygen atoms in SAMs derived from **1** and **1′** are closer to the surface than the terminal oxygen is SAMs derived from ethoxyethylene glycol. Moveover, the advancing contact

TABLE 4 Amount of Adsorbed Fibrinogen on SAMs Normalized to the Amount of Fibrinogen Adsorbed on a Monolayer of Hexadecanethiol [19]

Adsorbate[a]	% Protein adsorption (±2)
1 or 1′	56
2 or 2′	68
3 or 3′	87

[a]No "odd–even" effects were observed.

angle of water on SAMs derived from **1** and **1′** (∼68°) is closer to that observed from methoxy-terminated OEG SAMs (∼65°) than it is for ethoxy-terminated OEG SAMs (∼84°). Given, however, that the presence of water—either as a thin layer on top of the film or intercalated into the film—is required for efficient protein resistance [19], it is possible that the unexpectedly low fibrinogen resistance of SAMs derived from **1** and **1′** arises from the poor inner hydrophilicity of these SAMs, which discourages the intercalation of water. To confirm this hypothesis, additional studies involving a wider variety of proteins and substrates will be examined.

CONCLUSIONS

Six new cyclic acetal-terminated alkanethiols were synthesized and used to generate SAMs on gold. The new SAMs were characterized by ellipsometry, contact-angle goniometry, and PM-IRRAS. These surfaces were compared with ones generated from surface-grafted PEG and from OEG-terminated thiols. All of the analyses indicate that the new adsorbates form densely packed and conformationally ordered monolayer films. Furthermore, the wettability data suggest that adsorbates **1**, **1′**, **2**, and **2′** generate surfaces similar in energy to methoxy-terminated OEG SAMs and surface-grafted PEG; in contrast, adsorbates **3** and **3′** generate surfaces that are substantially more hydrophobic (*i.e.*, lower surface free energy). As a consequence, we anticipated that SAMs derived from **1**, **1′**, **2**, and **2′** would exhibit some kind of protein resistance, whereas those derived from **3** and **3′** would likely be protein adsorbers. Indeed, our preliminary studies of protein resistance utilizing fibrinogen as a model protein confirmed these assumptions, and a trend was observed with **1** and **1′** being the most protein-resistant adsorbate and **3** and **3′** the least. These studies support the importance of the hydrophilicity of the terminal group: as the oxygen atoms are buried into the film, the surface becomes less resistant to protein adsorption. Finally, comparison of our data with that obtained for the adsorption of fibrinogen on OEG SAMs suggests that the intercalation of water into the film is also critical for effecting protein resistance.

REFERENCES

[1] Harris, J. M. and Zalipsky, S., *Poly(ethylene glycol) Chemistry and Biological Applications* (American Chemical Society, Washington DC, 1997).

[2] Roberts, C., Chen, C. S., Mrksich, M., Martichonok, V., Ingber, D. E., and Whitesides, G. M., *J. Am. Chem. Soc.* **120**, 6548–6555 (1998).

[3] Mrksich, M., *Cell. Mol. Life Sci.*, **54**, 653–662 (1998).
[4] Ratner, B. D., Hoffmann, F. J., Schoen, J. E., and Lemons, F., *Biomaterials Science. An Introduction to Materials in Medicine* (Academic Press, New York, 1996).
[5] Jeon, S. I., Lee, J. H., Andrade, J. D., and De Gennes, P. G., *J. Colloid Interface Sci.* **142**, 149–158 (1991).
[6] Pale-Grosdemange, C., Simon, E. S., Prime, K. L., and Whitesides, G. M., *J. Am. Chem. Soc.* **113**, 12–20 (1991).
[7] Prime, K. L. and Whitesides, G. M., *J. Am. Chem. Soc.* **115**, 10714–10721 (1993).
[8] Zhu, B., Eurell, T., Gunawan, R., and Leckband, D., *J. Biomed. Mat. Res.* **56**, 406–416 (2001).
[9] Harder, P., Grunze, M., Dahint, R., Whitesides, G. M., and Laibinis, P. E., *J. Phys. Chem. B* **102**, 426–436 (1998).
[10] Benesch, J., Svedhem, S., Svensson, S., Valiokas, R., Liedberg, B., and Tengvall, P., *J. Biomater. Sci. Polymer Ed.* **12**, 581–597 (2001).
[11] Sofia, S. J., Premnath, V., and Merrill, E. W., *Macromolecules* **31**, 5059–5070 (1998).
[12] Tokumitsu, S., Liebich, A., Herrwerth, S., Eck, W., Himmelhaus, M., and Grunze, M., *Langmuir* **18**, 8862–8870 (2002).
[13] Milner, S. T., *Science* **251**, 905–914 (1991).
[14] Halperin, A., *Langmuir* **15**, 2525–2533 (1999).
[15] Zwahlen, M., Herrwerth, S., Eck, W., Grunze, M., and Hahner, G., *Langmuir* **19**, 9305–9310 (2003).
[16] Zdyrko, B., Varshney, S. K., and Luzinov, I., *Langmuir* **20**, 6727–6735 (2004).
[17] Ulman, A., *Chem. Rev.* **96**, 1533–1554 (1996).
[18] Tao, Y.-T., *J. Am. Chem. Soc.* **115**, 4350–4358 (1993).
[19] Herrwerth, S., Eck, W., Reinhardt, S., and Grunze, M., *J. Am. Chem. Soc.* **125**, 9359–9366 (2003).
[20] Wenzl., I., Yam, C. M., Barriet, D., and Lee, T. R., *Langmuir* **19**, 10217–10224 (2003).
[21] Whitesides, G. M. and Laibinis, P. E., *Langmuir* **6**, 87–96 (1990).
[22] Miura, Y. F., Takenaga, M., Koini, T., Graupe, M., Garg, N., Graham Jr., R. L., and Lee, T. R., *Langmuir* **14**, 5821–5825 (1998).
[23] Xia, N., Hu, Y., Grainger, D. W., and Castner, D. G., *Langmuir* **18**, 3255–3262 (2002).
[24] Colorado, R., Jr. and Lee, T. R., *J. Phys. Org. Chem.* **13**, 796–807 (2000).
[25] Bain, C. D., Throughton, E. B., Tao, Y.-T., Evall, J., Whitesides, G. M., and Nuzzo, R. G., *J. Am. Chem. Soc.* **111**, 321–335 (1989).
[26] Good, R. J. and Girifalco, L. A., *J. Physical Chem.* **64**, 561–565 (1960).
[27] Fowkes, F. M., *J. Physical Chem.* **67**, 2538–2541 (1963).
[28] Dann, J. R., *J. Coll. Interface Sci.* **32**, 302–320 (1970).
[29] Dann, J. R., *J. Coll. Interface Sci.* **32**, 321–331 (1970).
[30] Colorado, R., Jr. and Lee, T. R., *Langmuir* **19**, 3288–3296 (2003).
[31] Nuzzo, R. G., Dubois, L. H., and Allara, D. L., *J. Am. Chem. Soc.* **112**, 558–569 (1990).
[32] Roeges, N. P. G., *A Guide to the Complete Interpretation of Infrared Spectra of Organic Structures* (Wiley, New York, 1994).
[33] Lin-Vien, D., Colthup, N. B., Fateley, W. G., and Grasselli, J. G., *The Handbook of Infrared and Raman Characteristic Frequncies of Organic Molecules* (Academic Press, San Diego, 1991).
[34] Ulman, A. and Lee, E. F., *Characterization of Organic Thin Films* (Butterworth-Heinemann, Stoneham, MA: 1995).
[35] Zheng, J., Li, L., Chen, S., and Jiang, S., *Langmuir* **20**, 8931–8938 (2004).